

# The influence of triplet energy levels of bridging ligands on energy transfer processes in Ir(III)/Eu(III) dyads†

Weili Jiang,<sup>a</sup> Bin Lou,<sup>a</sup> Jianqiang Wang,<sup>b</sup> Hongbin Lv,<sup>a</sup> Zuqiang Bian\*<sup>a</sup> and Chunhui Huang<sup>a</sup>

Received 24th May 2011, Accepted 10th August 2011

DOI: 10.1039/c1dt10968e

A series of N<sup>^</sup>N,O<sup>^</sup>O-bridging ligands based on substituted 1-(pyridin-2-yl)-3-methyl-5-pyrazolone and their corresponding heteroleptic iridium(III) complexes as well as Ir–Eu bimetallic complexes were synthesized and fully characterized. The influence of the triplet energy levels of the bridging ligands on the energy transfer (ET) process from the Ir(III) complexes to Eu(III) ions in solution was investigated at 77 K in Ir(III)/Eu(III) dyads. Photophysical experiment results show the bridging ligands play an important role in the ET process. Only when the triplet energy level of the bridging ligand was lower than the triplet metal-to-ligand charge transfer (<sup>3</sup>MLCT) energy level of the Ir moiety, was pure emission from the Eu(III) ion observed, implying complete ET took place from the Ir moiety to the Eu(III) ion.

## Introduction

Europium(III) complexes attract considerable interest as analytical sensors,<sup>1–7</sup> biological labels<sup>8–12</sup> and luminescent materials for organic light-emitting diodes,<sup>13–19</sup> due to their unique narrow emission, large Stokes shifts and long luminescent lifetimes.<sup>20,21</sup> Since the f–f absorption of lanthanides is very weak, indirect excitation (termed “antenna effect”) is used to enhance the luminescence intensity.<sup>22</sup> For example, heterocyclic β-diketones such as 1-phenyl-3-methyl-4-acyl-5-pyrazolones<sup>23,24</sup> and 3-phenyl-4-acyl-5-isoxazolones<sup>25–27</sup> have been successfully employed as sensitizers for Eu(III) ions and Tb(III) ions. To design and synthesize effective organic ligands (antennae) for sensitizing europium ions, much effort has been devoted to understanding the correlation between the lowest triplet energy level of the organic ligand and the <sup>5</sup>D<sub>3</sub> levels of the Eu(III) ion.<sup>24,28–31</sup>

In this decade, transition metal-based ligands have received an increasing amount of attention as antennae<sup>32–46</sup> because of their ability to achieve sensitization at longer wavelengths. Iridium(III) complexes exhibit a significant advantage for sensitizing Eu(III) ions by their tunable metal-to-ligand charge-transfer (MLCT) transitions and the strong spin-orbit coupling of the iridium ion.<sup>47</sup> De Cola *et al.* first used 5-(2-pyridinyl)-1,2,4-triazole-3-carboxylic acid as a linking ligand between Ir and Eu moieties; white (mixed cyan and red) emission was

observed from this bimetallic complex in solution due to partial energy transfer from the excited Ir(III) center to the Eu(III) ion.<sup>41</sup> Recently, our group synthesized an Ir–Eu bimetallic complex containing the novel linking ligand 4,4,5,5,5-pentafluoro-1-(1',10'-phenanthrolin-2'-yl)pentane-1,3-dione (phen5f). Complete energy transfer (ET) from the Ir(III) moiety to Eu(III) occurred, leading to pure red emission from the Eu(III) ion.<sup>42</sup> The different results obtained for these two complexes can be ascribed to the distinct linking ligands. Recently, we reported that the cyclometalating ligand (2,4-difluoro)phenylpyridine (dfppy) in such cyclometalated iridium complexes is more suitable to sensitize Eu(III) ions than ppy (1-phenylpyridine).<sup>48</sup> However, as far as we know, no work has been published which systematically investigates the influence of the linking ligand on the ET process in Ir–Eu bimetallic complexes. Our previous work showed that phen5f itself might participate in the charge transfer (CT) process,<sup>49,50</sup> making the ET process more difficult to isolate. To better understand the effect of the linking ligand on the ET process, a series of N<sup>^</sup>N,O<sup>^</sup>O-linking ligands based on 1-(pyridin-2-yl)-3-methyl-5-pyrazolone with tunable triplet energy levels were designed and synthesized. Most importantly, such ligands do not participate in the CT process according to previous research.<sup>51</sup> The corresponding heteroleptic iridium complexes of the ligands as well as Ir–Eu bimetallic complexes were synthesized with dfppy as the cyclometalating ligand. Photophysical studies of the free ligands and their corresponding complexes show that the linking ligands behave as ET channels between the Ir and Eu centers, and the triplet energy levels of these ligands are the key for facile ET.

## Experimental

### Methods and instruments

<sup>1</sup>H NMR spectra were recorded on a Bruker ARX-400 NMR spectrometer. Chemical shift data are reported in ppm with

<sup>a</sup>Beijing National Laboratory for Molecular Sciences, State Key Laboratory of Rare Earth Materials Chemistry and Applications, College of Chemistry and Molecular Engineering, Peking University, Beijing, 100871, China. E-mail: bianzq@pku.edu.cn; Fax: (+86) 10-6275-7156; Tel: (+86) 10-6275-3544

<sup>b</sup>Shanghai Synchrotron Radiation Facility, Shanghai Institute of Applied Physics, Chinese Academy of Sciences, Shanghai, 201204, P. R. China

† Electronic supplementary information (ESI) available. CCDC reference numbers 827105, 781690, 781691. For ESI and crystallographic data in CIF or other electronic format see DOI: 10.1039/c1dt10968e

tetramethylsilane as an internal reference. Elemental analyses (C, H, N) were performed on a Elementar Vario EL instrument. Mass spectra were recorded on a ZAB-HS mass spectrometer (MS) (EI) and a Bruker Apex IV FTMS high-resolution MS (HRMS, ESI+). UV-vis absorption spectra were measured on a Shimadzu UV-3100 spectrometer (Japan). Photoluminescence (PL) spectra were recorded on an Edinburgh Analytical Instruments FLS920 spectrometer (United Kingdom). Luminescence quantum yields ( $\Phi$ ) were measured using [(dippy)<sub>2</sub>Ir(pic)] ( $\Phi = 0.42$ ) as a reference.<sup>52</sup> Melting points (m.p.) were measured on an X4 melting point apparatus. The solvents used in photophysical experiments were of spectroscopic grade. X-ray diffraction data were collected on a Rigaku MicroMax-007 CCD diffractometer (Japan) using graphite-monochromated Mo/K $\alpha$  ( $\lambda = 0.71073 \text{ \AA}$ ) radiation. Full crystallographic data are provided.†The X-ray absorption data at the Eu  $L_3$ -edge were measured at room temperature in fluorescent mode with SDD detector at beam line BL14W of the Shanghai Synchrotron Radiation Facility (SSRF), China.

### Synthesis

All reagents and solvents were of analytical grade and used as received, except 1,4-dioxane, which was distilled from NaH prior to use. 3-Methyl-1-(pyridin-2-yl)-pyrazol-5-one (**1**),<sup>51</sup> **2a**<sup>51</sup> and [Ir(dfppy)<sub>2</sub>( $\mu$ -Cl)]<sub>2</sub> dimers (**3**)<sup>53,54</sup> were prepared according to reported procedures.

### General procedure for the synthesis of 3-methyl-1-(pyridin-2-yl)-4-(*R*-carbonyl)-pyrazol-5-one (**2b–2e**).<sup>24</sup>

1-(Pyridin-2-yl)-3-methyl-5-pyrazolone (**1**, 0.05 mol) and dry 1,4-dioxane (100 mL) were placed in a 250 mL flask with a magnetic stirrer and heated to 70 °C under a flow of nitrogen. After 10 min, calcium hydroxide (0.12 mol) and barium hydroxide (0.03 mol) were added to the solution, which was then cooled to room temperature. The corresponding acyl chloride (0.058 mol) was added dropwise, and the resulting mixture was heated under reflux for 6 h. After cooling to room temperature the mixture was poured into ice-cold water (400 mL). Hydrochloric acid (5 M) was added to adjust the pH to 2–3. The mixture was left to stand overnight, resulting in the formation of a precipitate. The precipitate was filtered and then recrystallized from ethanol.

### 3-Methyl-4-(benzylcarbonyl)-1-(pyridin-2-yl)-1*H*-pyrazol-5(4*H*)-one (**2b**)

Yield: 33%. M.p.: 136–138 °C. <sup>1</sup>H NMR (400 MHz, CDCl<sub>3</sub>):  $\delta$  8.30 (d, 1H,  $J = 5.1$  Hz), 7.93–7.94 (d, 2H), 7.29–7.36 (m, 4H), 7.21–7.25 (m, 2H), 4.18 (s, 2H), 2.47 (s, 3H). MS (EI):  $m/z$  202 ([M – benzyl]).

### 3-Methyl-4-(phenylcarbonyl)-1-(pyridin-2-yl)-1*H*-pyrazol-5(4*H*)-one (**2c**)

Yield: 35%. M.p.: 182–183 °C. <sup>1</sup>H NMR (400 MHz, CDCl<sub>3</sub>):  $\delta$  8.26 (d, 1H,  $J = 5.0$  Hz), 7.93–8.00 (m, 2H), 7.81–7.84 (m, 2H), 7.57 (t, 1H,  $J = 8.0$  Hz), 7.46–7.49 (m, 2H), 7.24 (ddd, 1H,  $J = 9.9, 7.4, 1.6$  Hz), 2.51 (s, 3H). MS (EI):  $m/z$  278 ([M – H]).

### 3-Methyl-4-(4-fluorobenzylcarbonyl)-1-(pyridin-2-yl)-1*H*-pyrazol-5(4*H*)-one (**2d**)

Yield: 43%. M.p.: 196–197 °C. <sup>1</sup>H NMR (400 MHz, CDCl<sub>3</sub>):  $\delta$  8.26 (d, 1H,  $J = 5.0$  Hz), 7.94–8.00 (m, 2H), 7.83–7.88 (m, 2H), 7.25 (dd, 1H,  $J = 5.8$  Hz), 7.14 (m, 2H), 2.51 (s, 3H), MS (EI):  $m/z$  296 ([M – H]).

### 3-Methyl-4-(2-naphthylcarbonyl)-1-(pyridin-2-yl)-1*H*-pyrazol-5(4*H*)-one (**2e**)

Yield: 38%. M.p.: 199–200 °C. <sup>1</sup>H NMR (400 MHz, CDCl<sub>3</sub>):  $\delta$  8.35 (s, 1H), 7.99 (d, 1H,  $J = 5.0$  Hz), 7.89–8.01 (m, 6H), 7.50–7.59 (m, 2H), 7.22 (dd, 1H,  $J = 6.0$  Hz), 2.54 (s, 3H). MS (EI):  $m/z$  328 ([M – H]).

### General procedure for the synthesis of iridium complexes **4a–4e**

[Ir(dfppy)<sub>2</sub>( $\mu$ -Cl)]<sub>2</sub> (**3**, 0.2 mmol, 1 equiv.), sodium carbonate (1.0 mmol, 5 equiv.) and **2a–2e** (0.44 mmol, 2.2 equiv.) were stirred in ethylene glycol (30 mL) at 90 °C for 12 h under nitrogen. After the solvent was removed under reduced pressure, the resulting yellow solid was purified by column chromatography (CC) on silica gel and then recrystallized from CH<sub>2</sub>Cl<sub>2</sub>/*n*-hexane.

### [(dfppy)<sub>2</sub>Ir(mpfpCF<sub>3</sub>)] (**4a**)

CC: dichloromethane/petroleum ether (10:1, v/v). Yield: 71%. Anal. calcd. for C<sub>33</sub>H<sub>19</sub>F<sub>7</sub>IrN<sub>5</sub>O<sub>2</sub>·1/2C<sub>4</sub>H<sub>8</sub>O<sub>2</sub>: C, 47.40; H, 2.61; N, 7.90; found: C, 47.63; H, 2.40; N, 8.10. FT-IR:  $\nu = 3070$  (m); 2927 (m); 1692(m), 1636 (s); 1600 (vs); 1570 (s); 1470 (vs); 1296 (m); 1153 (s); 986 (m); 823 (s); 764 (s) cm<sup>-1</sup>. <sup>1</sup>H NMR (400 MHz, CDCl<sub>3</sub>):  $\delta$  9.07 (d, 1H,  $J = 8.6$  Hz), 8.34 (d, 1H,  $J = 8.7$  Hz), 8.30 (d, 1H,  $J = 8.6$  Hz), 8.16 (d, 1H,  $J = 5.5$  Hz), 7.80–7.87 (m, 3H), 7.54 (d, 1H,  $J = 5.5$  Hz), 7.45 (d, 1H,  $J = 4.8$  Hz), 7.18 (t, 1H,  $J = 6.1$  Hz), 7.04 (t, 1H,  $J = 6.2$  Hz), 6.93 (t, 1H,  $J = 6.2$  Hz), 6.45–6.56 (m, 2H), 6.62 (ddd, 2H,  $J = 8.3, 8.3, 2.3$  Hz), 1.94 (s, 3H). HRMS (ESI+, MeOH): calcd. for C<sub>33</sub>H<sub>20</sub>F<sub>7</sub>IrN<sub>5</sub>O<sub>2</sub>, 844.1129 ([M+H]<sup>+</sup>); found, 844.1114.

### [(dfppy)<sub>2</sub>Ir(mpfpBe)] (**4b**)

CC: ethyl acetate/petroleum ether (2:1 v/v). Yield: 67%. Anal. calcd. for C<sub>39</sub>H<sub>26</sub>F<sub>4</sub>IrN<sub>5</sub>O<sub>2</sub>: C, 54.10; H, 3.14; N, 8.09; found: C, 54.14; H, 2.94; N, 8.02. FT-IR:  $\nu = 3082$  (m); 2925 (w); 1656 (m); 1601 (vs); 1574 (s); 1463 (s); 1294 (m); 1106 (w); 986 (m); 826 (m); 760 (w) cm<sup>-1</sup>. <sup>1</sup>H NMR (400 MHz, CDCl<sub>3</sub>):  $\delta$  9.11 (d, 1H,  $J = 8.6$  Hz), 8.28–9.00 (m, 2H), 8.13 (d, 1H,  $J = 5.7$  Hz), 7.79–7.83 (m, 3H), 7.55 (d, 1H,  $J = 5.7$  Hz), 7.44 (d, 1H,  $J = 5.6$  Hz), 7.36 (d, 2H,  $J = 8.0$  Hz), 7.27–7.29 (m, 2H), 7.08–7.20 (m, 2H), 7.01 (t, 1H,  $J = 5.8$  Hz), 6.90 (t, 1H,  $J = 5.9$  Hz), 6.37–6.52 (m, 2H), 5.59–5.64 (m, 2H), 4.32 (s, 2H), 1.89 (s, 3H). HRMS (ESI+, MeOH): calcd. for C<sub>39</sub>H<sub>27</sub>F<sub>4</sub>IrN<sub>5</sub>O<sub>2</sub>, 866.1725 ([M+H]<sup>+</sup>); found, 866.1735.

### [(dfppy)<sub>2</sub>Ir(mpfpPh)] (**4c**)

CC: ethyl acetate/petroleum ether (2:1 v/v). Yield: 69%. Anal. calcd. for C<sub>38</sub>H<sub>24</sub>F<sub>4</sub>IrN<sub>5</sub>O<sub>2</sub>·1/2H<sub>2</sub>O: C, 53.08; H, 2.93; N, 8.14; found: C, 53.01; H, 2.86; N, 7.83. FT-IR:  $\nu = 3090$  (m); 2982 (w); 1654 (m); 1601 (vs); 1571 (s); 1472 (s); 1430 (s); 1294 (m); 1107 (m); 985 (m); 822 (w); 753 (m) cm<sup>-1</sup>. <sup>1</sup>H NMR (400 MHz, CDCl<sub>3</sub>):

$\delta$  9.01 (d, 1H,  $J = 8.6$  Hz), 8.37 (d, 1H,  $J = 7.6$  Hz), 8.31 (d, 1H,  $J = 7.5$  Hz), 8.23 (d, 1H,  $J = 5.0$  Hz), 7.83–7.85 (m, 2H), 7.72–7.76 (m, 3H), 7.60 (d, 1H,  $J = 5.1$  Hz), 7.38–7.45 (m, 4H), 7.18 (t, 1H,  $J = 6.0$  Hz), 7.04 (t, 1H,  $J = 6.0$  Hz), 6.87 (t, 1H,  $J = 6.0$  Hz), 6.47–6.52 (m, 2H), 5.62–5.67 (m, 2H), 1.96 (s, 3H). HRMS (ESI+, MeOH): calcd. for  $C_{38}H_{25}F_4IrN_5O_2$ , 852.1568 ( $[M+H]^+$ ); found, 852.1555.

#### **[(dfppy)<sub>2</sub>Ir(mpfpPhF)] (4d)**

CC: ethyl acetate/petroleum ether (2:1 v/v). Yield: 63%. Anal. calcd. for  $C_{38}H_{23}F_5IrN_5O_2 \cdot 1/2C_4H_8O_2$ : C, 52.63; H, 2.98; N, 7.67; found: C, 52.40; H, 2.76; N, 7.56. FT-IR:  $\nu = 3063$  (w); 2980 (w); 1657 (s); 1603 (vs); 1574 (s); 1469 (s); 1436 (s); 1226 (m); 1294 (w); 1105 (m); 987 (w); 844 (w); 761 (m)  $cm^{-1}$ .  $^1H$  NMR (400 MHz,  $CDCl_3$ ):  $\delta$  9.01 (d, 1H,  $J = 8.7$  Hz), 8.35 (d, 1H,  $J = 7.4$  Hz), 8.28 (d, 1H,  $J = 7.5$  Hz), 8.21 (d, 1H,  $J = 4.9$  Hz), 7.76–7.84 (m, 5H), 7.59 (d, 1H,  $J = 5.0$  Hz), 7.45 (d, 1H,  $J = 5.7$  Hz), 7.18 (t, 1H,  $J = 5.4$  Hz), 7.02–7.09 (m, 3H), 6.89 (t, 1H,  $J = 6.2$  Hz), 6.40–6.53 (m, 2H), 5.62–5.65 (m, 2H), 1.95 (s, 3H). HRMS (ESI+, MeOH) calcd. for  $C_{38}H_{24}F_5IrN_5O_2$ , 870.1474 ( $[M+H]^+$ ); found, 870.1468.

#### **[(dfppy)<sub>2</sub>Ir(mpfpNaph)] (4e)**

CC: ethyl acetate/petroleum ether (2:1 v/v). Yield: 72%. Anal. calcd. for  $C_{42}H_{26}F_4IrN_5O_2 \cdot 1/2H_2O$ : C, 55.44; H, 2.99; N, 7.70; found: C, 55.55; H, 2.76; N, 7.75. FT-IR:  $\nu = 3062$  (w); 1654 (m); 1598 (vs); 1574 (s); 1464 (s); 1434 (s); 1294 (m); 1107 (m); 985 (m); 817 (m); 756 (m)  $cm^{-1}$ .  $^1H$  NMR (400 MHz,  $CDCl_3$ ):  $\delta$  9.01 (d, 1H,  $J = 8.6$  Hz), 8.37 (d, 1H,  $J = 8.8$  Hz), 8.26–8.31 (m, 3H), 7.92 (d, 1H,  $J = 7.6$  Hz), 7.82–7.88 (m, 5H), 7.73 (t, 1H,  $J = 8.0$  Hz), 7.62 (d, 1H,  $J = 5.0$  Hz), 7.44–7.51 (m, 3H), 7.21 (t, 1H,  $J = 5.9$  Hz), 7.06 (t, 1H,  $J = 6.0$  Hz), 6.87 (t, 1H,  $J = 6.0$  Hz), 6.48–6.53 (m, 2H), 5.63–5.69 (m, 2H), 1.99 (s, 3H). HRMS (ESI+, MeOH) calcd. for  $C_{42}H_{27}F_4IrN_5O_2$ , 902.1725 ( $[M+H]^+$ ); found, 902.1713.

#### **General procedure for the synthesis of bimetallic Ir–Eu complexes 5a–5e**

Iridium complex (**4a–4e**, 0.3 mmol, 1 equiv.) and  $EuCl_3 \cdot 6H_2O$  (0.1 mmol, 0.33 equiv.) were stirred in ethanol (30 mL) under reflux for 6 h, when a clear solution was obtained. The final corresponding binuclear complexes were recrystallized from  $CH_2Cl_2/n$ -hexane.

#### **[(dfppy)<sub>2</sub>Ir(mpfpCF<sub>3</sub>)<sub>3</sub>EuCl]Cl<sub>2</sub> (5a)**

Anal. calcd. for  $C_{99}H_{57}Cl_3EuF_{21}Ir_3N_{15}O_6 \cdot 3C_2H_5OH$ : C, 43.12; H, 2.58; N, 7.18; found: C, 42.75; H, 2.96; N, 7.44. FT-IR:  $\nu = 3090$  (w); 1685(m), 1639 (s); 1600 (vs); 1570 (s); 1470 (vs); 1294(m); 1154 (s); 986 (m); 825 (s); 763 (s)  $cm^{-1}$ . HRMS (ESI+, MeOH): calcd. for  $C_{66}H_{38}Cl_2EuF_{14}Ir_2N_{14}O_4$ , 1909.0678 ( $[M-4a-Cl]^+$ ); found, 1909.0688.

#### **[(dfppy)<sub>2</sub>Ir(mpfpBe)<sub>3</sub>EuCl]Cl<sub>2</sub> (5b)**

Anal. calcd. for  $C_{117}H_{78}Cl_3EuF_{12}Ir_3N_{15}O_6 \cdot 2C_2H_5OH$ : C, 49.35; H, 3.08; N, 7.13; found: C, 49.28; H, 3.31; N, 7.41. FT-IR:  $\nu = 3500$ –2900 (m); 1650 (m); 1601 (vs); 1574 (s); 1470 (s); 1295 (m); 1106 (w); 986 (m); 826 (m); 760 (w)  $cm^{-1}$ . HRMS (ESI+, MeOH): calcd. for  $C_{78}H_{52}Cl_2EuF_8Ir_2N_{10}O_4$ , 1953.1904 ( $[M-4b-Cl]^+$ ); found, 1953.1990.

#### **[(dfppy)<sub>2</sub>Ir(mpfpPh)<sub>3</sub>EuCl]Cl<sub>2</sub> (5c)**

Anal. calcd. for  $C_{114}H_{72}Cl_3EuF_{12}Ir_3N_{15}O_6 \cdot 3H_2O$ : C, 47.79; H, 2.74; N, 7.33; found: C, 47.50; H, 3.17; N, 7.23. FT-IR:  $\nu = 3500$ –2900 (m); 1639 (m); 1600 (vs); 1571 (s); 1472 (vs); 1431 (s); 1296 (m); 1107 (m); 987 (m); 826 (w); 759 (m)  $cm^{-1}$ . HRMS (ESI+, MeOH): calcd. for  $C_{114}H_{72}Cl_2EuF_{12}Ir_3N_{15}O_6$ , 2774.3050 ( $[M-Cl]^+$ ); found, 2774.3128.

#### **[(dfppy)<sub>2</sub>Ir(mpfpPhF)<sub>3</sub>EuCl]Cl<sub>2</sub> (5d)**

Anal. calcd. for  $C_{114}H_{69}Cl_3EuF_{15}Ir_3N_{15}O_6 \cdot 2C_2H_5OH$ : C, 47.93; H, 2.76; N, 7.11; found: C, 48.02; H, 2.99; N, 7.33. FT-IR:  $\nu = 3062$  (w); 1656 (s); 1602 (vs); 1575 (s); 1468 (s); 1434 (s); 1222 (m); 1294 (w); 1106 (m); 987 (w); 845 (w); 763 (m)  $cm^{-1}$ . HRMS (ESI+, MeOH): calcd. for  $C_{114}H_{69}Cl_2EuF_{15}Ir_3N_{15}O_6$ , 2830.2793 ( $[M-Cl]^+$ ); found, 2830.2622.

#### **[(dfppy)<sub>2</sub>Ir(mpfpNaph)<sub>3</sub>EuCl]Cl<sub>2</sub> (5e)**

Anal. calcd. for  $C_{126}H_{78}Cl_3EuF_{12}Ir_3N_{15}O_6 \cdot 2H_2O$ : C, 50.49; H, 2.76; N, 7.01; found: C, 50.31; H, 3.06; N, 7.03. FT-IR:  $\nu = 3500$ –2900 (m); 1639 (m); 1599 (vs); 1574 (s); 1470 (s); 1430 (s); 1295 (m); 1108 (m); 986 (m); 826 (m); 758 (m)  $cm^{-1}$ . HRMS (ESI+, MeOH): calcd. for  $C_{126}H_{78}Cl_2EuF_{12}Ir_3N_{15}O_6$ , 2926.3556 ( $[M-Cl]^+$ ); found, 2926.2947.

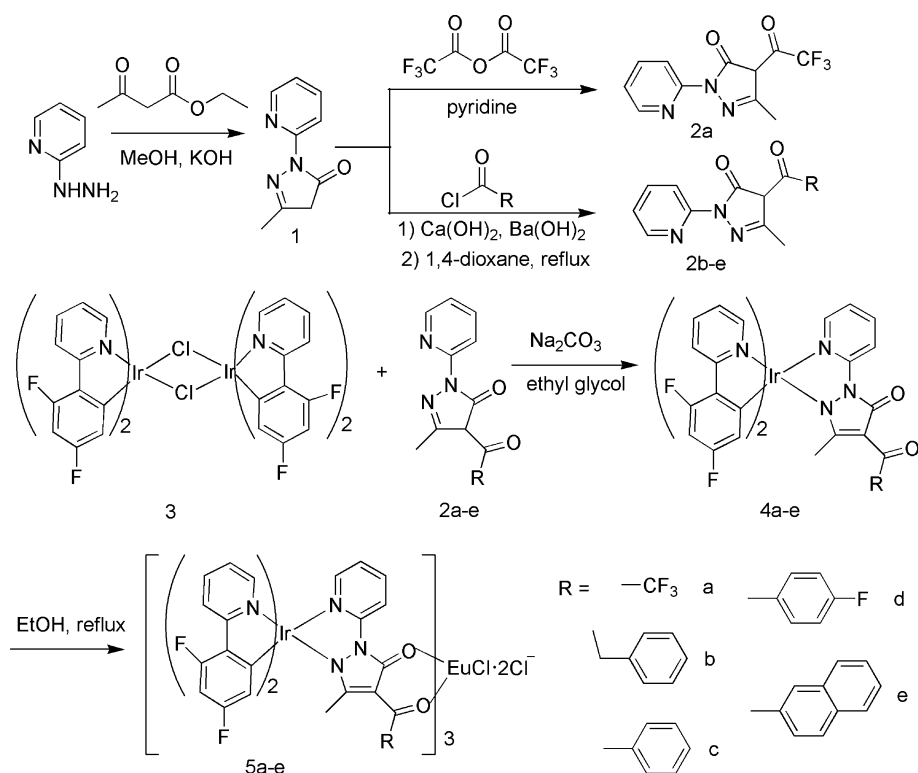
## **Results and discussion**

### **Synthesis and characterization**

Scheme 1 shows the general method to synthesize the  $N^{\wedge}N,O^{\wedge}O$ -linking ligands **2a–2e**, their corresponding iridium complexes **4a–4e** as well as Ir–Eu bimetallic complexes **5a–5e**. Linking ligands **2b–2e** were synthesized in two steps. Firstly, 2-hydrazinylpyridine was reacted with ethyl acetoacetate to form 3-methyl-1-(pyridin-2-yl)-pyrazol-5-one (**1**). **1** was then treated with the corresponding substituted acyl chloride in basic media, giving **2b–2e** in 33–43% yield. Each ligand was stirred with dichloro-bridged iridium dimer **3** in a solution of ethylene glycol at 90 °C for 12 h under nitrogen to form the corresponding Ir(III) complex. The crude products were purified by CC using silica gel, affording complexes **4a–4e** in 60–70% yield. A higher reaction temperature would decrease the yield. The final bimetallic Ir–Eu complexes (**5a–5e**) were obtained by refluxing  $EuCl_3 \cdot 6H_2O$  with the corresponding iridium complex in ethanol with a stoichiometric ratio of 1:3 (Eu/Ir). The products were characterized by elemental analysis, FT-IR absorptions,  $^1H$  NMR spectroscopy and HRMS.

### **X-ray crystal structures for iridium complexes**

Single crystals of complexes **4a**, **4b** and **4d** were obtained by slow evaporation of solvents from their dichloromethane/*n*-hexane solutions, and analyzed by X-ray crystallography. Crystal data and structure refinement for **4a**, **4b** and **4d** are summarized in Table 1. As shown in Fig. 1, the coordinated atoms are arranged as distorted octahedron around the central iridium atom in all of the complexes. The  $N^{\wedge}N$  site of the chelating linking ligand coordinates to the soft Ir ion in a bidentate fashion, leaving the  $O^{\wedge}O$  site free, which prefers to binding with  $Eu^{3+}$  ions. The two oxygen atoms in each linking ligand adopt a *trans* configuration



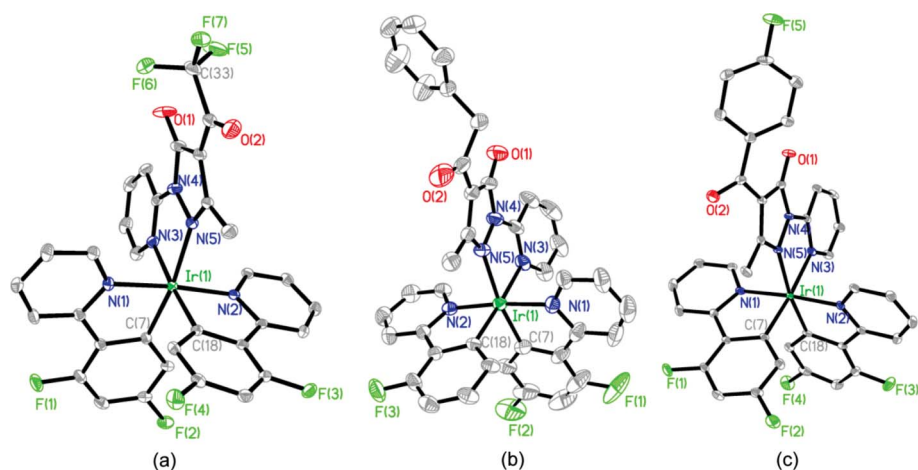
Scheme 1 General synthesis of the complexes reported in this work.

Table 1 Crystal data and structure refinement for **4a**·2C<sub>2</sub>H<sub>5</sub>OH, **4b** and **4d**·CH<sub>2</sub>Cl<sub>2</sub>

Complex	<b>4a</b> ·2C <sub>2</sub> H <sub>5</sub> OH	<b>4b</b>	<b>4d</b> ·CH <sub>2</sub> Cl <sub>2</sub>
Empirical formula	C <sub>37</sub> H <sub>31</sub> F <sub>7</sub> IrN <sub>5</sub> O <sub>4</sub>	C <sub>39</sub> H <sub>26</sub> F <sub>4</sub> IrN <sub>5</sub> O <sub>2</sub>	C <sub>39</sub> H <sub>25</sub> Cl <sub>2</sub> F <sub>5</sub> IrN <sub>5</sub> O <sub>2</sub>
Formula weight	934.87	864.85	953.74
<i>T</i> /K	113(2)	113(2)	113(2)
Wavelength $\lambda$ /Å	0.71075	0.71075	0.71075
Crystal system	Monoclinic	Triclinic	Monoclinic
Space group	P <sub>1</sub> 2 <sub>1</sub> /n 1	P <sub>-1</sub>	P <sub>1</sub> 2 <sub>1</sub> /n 1
<i>a</i> /Å	16.912(2)	11.4430(11)	12.5020(14)
<i>b</i> /Å	22.958(3)	17.2090(17)	21.921(2)
<i>c</i> /Å	19.037(2)	17.9900(17)	12.6430(15)
$\alpha$ (°)	90	90.543(4)	90
$\beta$ (°)	107.182(3)	99.623(18)	96.317(3)
$\gamma$ (°)	90	103.398(18)	90
<i>V</i> /Å <sup>3</sup>	7061.5(14)	3393.4(6)	3443.9(6)
<i>Z</i>	8	4	4
$\rho$ (calcd.) (g cm <sup>-3</sup> )	1.759	1.693	1.839
Absorption coefficient/mm <sup>-1</sup>	3.867	4.000	4.105
<i>F</i> (000)	3680	1696	1864
Crystal size/mm	0.22 × 0.16 × 0.14	0.24 × 0.22 × 0.20	0.22 × 0.18 × 0.16
$\theta$ range (deg)	1.42–33.19	1.15–27.68	1.86–27.90
Reflections collected/unique	103513/26867 [ <i>R</i> (int) = 0.0620]	37298/15773 [ <i>R</i> (int) = 0.0376]	36392/8206 [ <i>R</i> (int) = 0.0684]
Data/restraints/parameters	26867/168/1087	15773/94/961	8206/18/510
GOF on <i>F</i> <sup>2</sup>	1.206	1.093	0.965
Final <i>R</i> indices [ <i>I</i> > 2 $\sigma$ ( <i>I</i> )]	<i>R</i> <sub>1</sub> = 0.0602, <i>wR</i> <sub>2</sub> = 0.0960	<i>R</i> <sub>1</sub> = 0.0441, <i>wR</i> <sub>2</sub> = 0.0902	<i>R</i> <sub>1</sub> = 0.0324, <i>wR</i> <sub>2</sub> = 0.0680
<i>R</i> indices (all data)	<i>R</i> <sub>1</sub> = 0.0726, <i>wR</i> <sub>2</sub> = 0.0998	<i>R</i> <sub>1</sub> = 0.0557, <i>wR</i> <sub>2</sub> = 0.0951	<i>R</i> <sub>1</sub> = 0.0402, <i>wR</i> <sub>2</sub> = 0.0705

as a lower energy arrangement, which are easy to turn to *cis*-configuration when coordinating to Eu<sup>3+</sup> ion.<sup>42,55</sup> Selected bond lengths and angles of the complexes are listed in Table 2. The dpfp ligands have Ir–N bonds of similar length (Ir(1)–N(1) and Ir(1)–N(2)) to those of the Ir–C bonds. The Ir–N bonds between Ir(III) and the linking ligand (Ir(1)–N(3) and Ir(1)–N(5)) are longer

than those of Ir(1)–N(1) and Ir(1)–N(2) because of the *trans* effect. The angles for N(1)–Ir(1)–C(7), N(2)–Ir(1)–C(18) and N(3)–Ir(1)–N(5) all deviate from 90°, while those for C(18)–Ir(1)–N(3), C(7)–Ir(1)–N(5) and N(1)–Ir(1)–N(2) (N(1)–Ir(1)–N(2), N(5)–Ir(1)–C(18) and N(3)–Ir(1)–C(7) for **4d**) deviate from 180°, confirming the Ir(III) ion is centered at a distorted octahedron.



**Fig. 1** Molecular structures of (a) **4a**, (b) **4b** and (c) **4d** with thermal ellipsoids drawn at the 30% probability level. Hydrogen atoms and solvent molecules are omitted for clarity.

**Table 2** Selected bond lengths (Å) and angles (°) in **4a**, **4b** and **4d**

Complex	<b>4a</b>	<b>4b</b>	<b>4d</b>
Ir(1)–N(1)	2.048(3)	2.058(4)	2.038(3)
Ir(1)–N(2)	2.045(3)	2.046(4)	2.035(3)
Ir(1)–N(3)	2.149(4)	2.156(4)	2.142(3)
Ir(1)–N(5)	2.126(4)	2.158(4)	2.118(3)
Ir(1)–C(7)	2.003(4)	2.012(5)	2.001(4)
Ir(1)–C(18)	2.017(4)	2.022(5)	2.009(4)
N(1)–Ir(1)–N(2)	174.87(14)	174.58(17)	175.22(11)
N(3)–Ir(1)–C(18)	175.76(15)	176.74(18)	171.54(12) <sup>a</sup>
N(5)–Ir(1)–C(7)	170.33(15)	169.97(19)	174.99(13) <sup>b</sup>
N(1)–Ir(1)–C(7)	80.41(16)	81.0(2)	80.35(13)
N(2)–Ir(1)–C(18)	80.65(15)	79.87(18)	80.60(14)
N(3)–Ir(1)–N(5)	76.65(14)	75.92(17)	75.64(11)

<sup>a</sup> this angle for **4d** is N(5)–Ir(1)–C(18); <sup>b</sup> this angle for **4d** is N(3)–Ir(1)–C(7)

### XAFS data analysis

The local structure of Eu(III) ions for the Ir–Eu bimetallic complexes was revealed by the analysis of the XAFS spectrum and **5e** was chosen as an example (Fig. 2).<sup>56</sup>  $\{[(dfppy)_2Ir(phen5f)]_3EuCl\}Cl_2$ <sup>42</sup> with a definite crystal structure was used as a reference. The Eu  $L_3$  - edge absorption spectra for **5e** and  $\{[(dfppy)_2Ir(phen5f)]_3EuCl\}Cl_2$  were plotted in Fig. 2a with a typical white-line peak at 6983 eV. The intensities of white-line peaks for **5e** and  $\{[(dfppy)_2Ir(phen5f)]_3EuCl\}Cl_2$  are very similar, indicating they have a similar coordinated structure. Further information on the coordinated environment around the metal center was provided by the analysis of EXAFS spectra (Fig. 2b). The fitting results of the EXAFS spectrum (Table S1†) of **5e** shows a coordination shell for Eu<sup>3+</sup> at 2.41 Å consists of six oxygen atoms from the carbonyl ligands, together with the chlorine backscatter at about 2.62 Å from the Eu–Cl contribution.

### Absorption spectra

The absorption spectra of complexes **4a–e** were recorded at room temperature in dichloromethane (Fig. 3). Intense bands ( $\epsilon \approx 2.0 \sim 8.5 \times 10^4 \text{ M}^{-1} \text{ cm}^{-1}$ ) at high energy (<340 nm) are assigned to spin-allowed  $\pi\text{--}\pi^*$  transitions localized on both dfppy and the

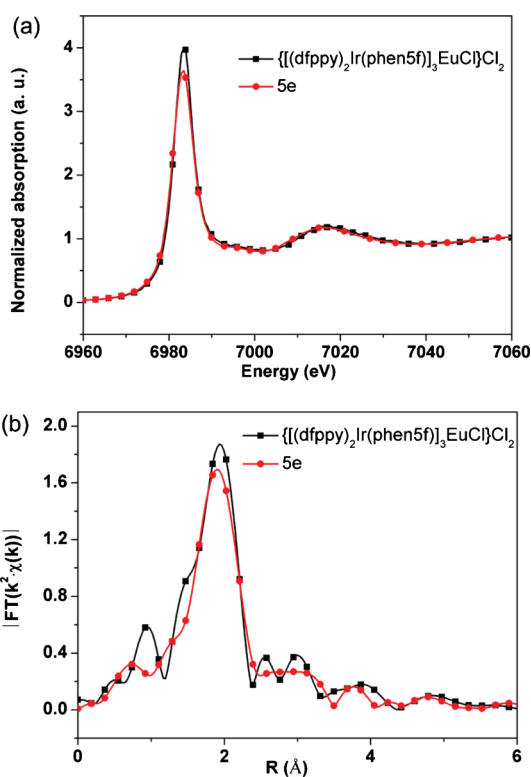


**Fig. 2** (a) Eu  $L_3$  - edge XANES spectra for **5e** and  $\{[(dfppy)_2Ir(phen5f)]_3EuCl\}Cl_2$ ; (b) Fourier transform of experimental data for **5e** and  $\{[(dfppy)_2Ir(phen5f)]_3EuCl\}Cl_2$  (without phase shift).

linking ligands. Weak absorptions ( $\epsilon \approx 1.0 \sim 2.0 \times 10^4 \text{ M}^{-1} \text{ cm}^{-1}$ ) at lower energy (340–400 nm) are attributed to spin-allowed singlet metal-to-ligand charge-transfer (<sup>1</sup>MLCT) transitions<sup>57</sup> from Ir(III) to dfppy. The major bands and their molar extinction coefficients are presented in Table 3. Complexes **4c–4e** show larger molar extinction coefficients than **4a–4b** for the band at approximately 360 nm, which can be attributed to the increased conjugation in **4c–4e**.

**Table 3** Photophysical spectral data for complexes **4a–4e**

Complex	Absorbance $\lambda$ (nm) <sup>a</sup> ( $\epsilon$ 10 <sup>4</sup> M <sup>-1</sup> cm <sup>-1</sup> )	Emission <sup>b</sup> $\lambda$ (nm) (rel. int.)	$\Phi^c$	Emission <sup>b</sup> $\lambda$ (nm) (rel. int.) at 77 K	$\tau_1$ ( $\mu$ s) ( $\chi^2$ ) at 77 K (450 nm)	$\tau_2$ ( $\mu$ s) ( $\chi^2$ ) at 77 K with EuCl <sub>3</sub> (450 nm)	$\tau_{Eu}$ ( $\mu$ s) ( $\chi^2$ ) at 77 K (614 nm)
<b>4a</b>	249(6.01), 291(sh, 3.05), 311(sh, 2.63), 336(2.02)	457 (0.99), 486 (1)	0.041	449 (1), 481 (0.71)	5.0 (1.02)	4.8 (1.04)	291 (1.31)
<b>4b</b>	248(6.24), 287(sh, 3.81), 350(1.22)	460 (1), 488 (0.98)	0.28	450 (1), 481 (0.72)	4.5(1.03)	3.5 (1.18)	258(1.25)
<b>4c</b>	243(6.60), 289(sh, 3.06), 322(sh, 2.15), 350(1.69)	463 (1), 487 (0.97)	0.022	450 (1), 481 (0.71)	4.4 (1.08)	2.8 (1.14)	276 (1.21)
<b>4d</b>	243(6.79), 290(sh, 3.11), 323(sh, 2.25), 354(1.87)	461 (0.99), 490 (1)	0.061	449 (1), 481 (0.71)	4.4 (1.06)	2.7 (1.19)	278 (1.27)
<b>4e</b>	244(8.23), 286(sh, 3.96), 310(sh, 2.42), 354(1.87)	—	—	490 (1), 527(0.73), 567 (0.24)	>1 ms (490 nm)	—	284 (1.23)

<sup>a</sup> 'sh' denotes a shoulder. <sup>b</sup>  $\lambda_{ex}$  = 360 nm. <sup>c</sup> Quantum yields are measured vs. (dippy)<sub>2</sub>Ir(pic), ( $\lambda_{ex}$  = 360 nm).<sup>52</sup>

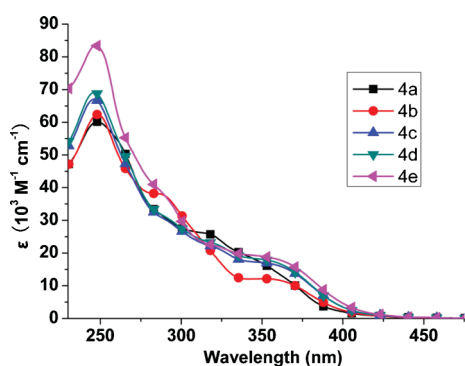


**Fig. 3** Absorption spectra of complexes **4a–4e** in CH<sub>2</sub>Cl<sub>2</sub> at room temperature.

#### Determination of the triplet energy levels of bridging ligands **2a–2e**

The triplet energy level of coordinated ligands is one of the most important factors in the ET pathway.<sup>28–30</sup> The lowest excited level of gadolinium (<sup>6</sup>P<sub>7/2</sub>–<sup>8</sup>S<sub>7/2</sub>) is located at 32150 cm<sup>-1</sup>, which is so high that it can be assumed that there is no ET between the central Gd(III) ion and its ligands. Besides, the triplet energy level of the ligand was not affected significantly by lanthanide ions. On this basis, the phosphorescence spectra of a gadolinium complex could be used to evaluate the triplet excited energy level of a corresponding coordinated ligand.<sup>24</sup> The phosphorescence spectra of ligands **2a–2e** were measured in a rigid matrix of EtOH at 77 K containing excess GdCl<sub>3</sub>·6H<sub>2</sub>O (Fig. 4). Under these conditions, all of the ligands in solution can be considered to coordinate with Gd<sup>3+</sup> ions. The triplet energy levels can thus be evaluated from the emission spectra. Using the wavelengths at half of the height of the emission band at shorter wavelength (**2a**, **2b**, **2c**, and **2d**) or the 0–0 transition (**2e**) in the corresponding phosphorescence spectra,<sup>24</sup> the triplet energy levels of **2a** to **2e** are estimated to be 2.26 × 10<sup>4</sup> cm<sup>-1</sup> (443 nm), 2.31 × 10<sup>4</sup> cm<sup>-1</sup> (432 nm), 2.24 × 10<sup>4</sup> cm<sup>-1</sup> (447 nm), 2.13 × 10<sup>4</sup> cm<sup>-1</sup> (469 nm) and 2.03 × 10<sup>4</sup> cm<sup>-1</sup> (492 nm), respectively. As expected, the triplet energy levels decrease (**2b** > **2a** > **2c** > **2d** > **2e**) as the conjugation increases, but all of the levels are higher than the <sup>5</sup>D<sub>0</sub> level of Eu<sup>3+</sup> (17500 cm<sup>-1</sup>).

#### Emission spectra of complexes **4a–4e**

The emission spectra of complexes **4a–4e** were measured at room temperature in dichloromethane under the same conditions. The results are shown in Fig. 5 and data are summarized in

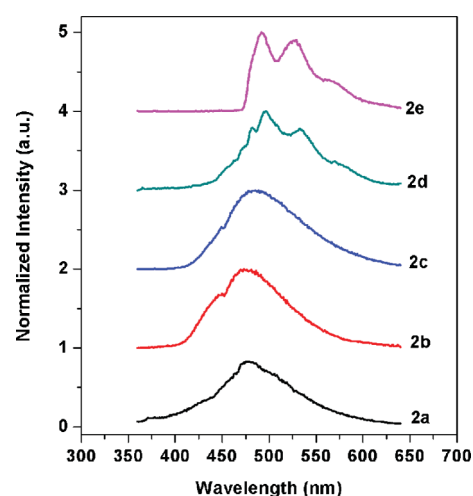


**Fig. 4** Emission spectra of **2a–2e** with excess GdCl<sub>3</sub>·6H<sub>2</sub>O at 77 K in EtOH glass (1 × 10<sup>-5</sup> M).

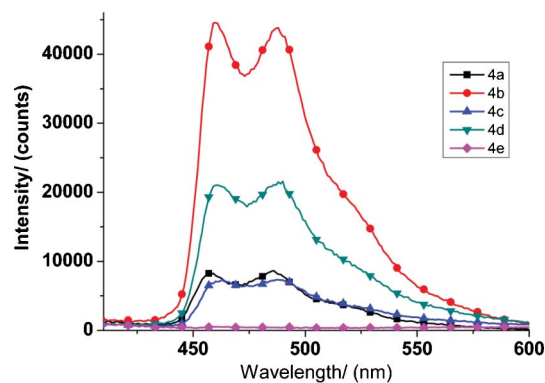


**Fig. 5** Emission spectra of **4a–4e** at room temperature in CH<sub>2</sub>Cl<sub>2</sub> (1 × 10<sup>-5</sup> M).

Table 3. The complexes exhibited photoluminescence with two peaks centered at *ca.* 460 and 490 nm, which is characteristic of <sup>3</sup>MLCT transitions of the (dfppy)<sub>2</sub>Ir<sup>+</sup> moiety,<sup>57</sup> suggesting that the linking ligands do not participate in the CT process. Another interesting phenomenon is that the intensity of luminescence (*i.e.*, the quantum yield) of **4a–4e** reflects the triplet energy levels of the linking ligands.<sup>58,59</sup> This indicates that the energy from the (dfppy)<sub>2</sub>Ir<sup>+</sup> moiety partly leaks to the linking ligands if the triplet energy level of the ligand is similar to or below the <sup>3</sup>MLCT level.<sup>52</sup>

Furthermore, the emission from  $^3\text{MLCT}$  transitions can be totally quenched when the triplet energy level of the linking ligand is low enough, such as in complex **4e**. Because the linking ligands are non-emissive at room temperature, any leaked energy is lost through non-radiative transitions.

Low-temperature emission spectra of the iridium complexes **4a–4e** were also measured at 77 K (Fig. 6 and Table 3). The phosphorescence spectra of **4a–4d** are similar both in shape and intensity, with two emission peaks centered at 450 and 481 nm. According to previous studies,<sup>57,59</sup> it can be concluded that the emission bands arise from the  $(\text{dfppy})_2\text{Ir}^+$  moiety, which has two main  $^3\text{MLCT}$  states at  $2.22 \times 10^4 \text{ cm}^{-1}$  ( $^3\text{MLCT}_1$ ) and  $2.08 \times 10^4 \text{ cm}^{-1}$  ( $^3\text{MLCT}_2$ ). As a result, significant ET can occur through “phonon-assisted energy transfer”,<sup>60–62</sup> which further confirms the presence of energy-leaking as discussed above. On the other hand, the lowest  $^3\text{MLCT}$  level ( $^3\text{MLCT}_2$ ) is lower in energy than the triplet energy levels of **4a–4d**, so there may also be ET from the triplet energy levels of **2a–2d** to  $^3\text{MLCT}_2$ . However, the spectrum of complex **4e** is quite different from those of **4a–4d**. Comparison of Fig. 6 with Fig. 4 shows that both the emissions arise from the triplet energy level of the free linking ligand **2e**. That is, in the excited states of complex **4e**, complete ET from  $(\text{dfppy})_2\text{Ir}$  to linking ligand **2e** occurs without reverse transfer because the triplet energy level of **2e** is lower than the  $^3\text{MLCT}_2$  level. This results in emissions only being observed from **2e**.

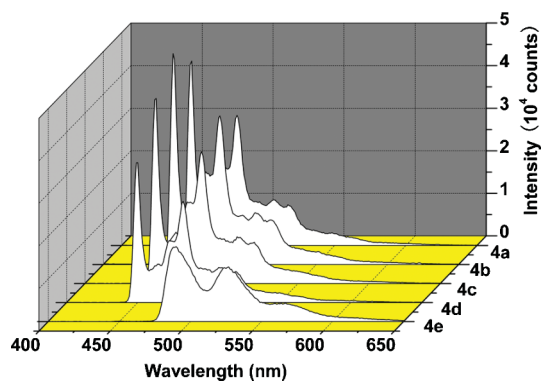


Fig. 6 Emission spectra of **4a–4e** at 77 K in EtOH glass ( $1 \times 10^{-5} \text{ M}$ ).

### ET in Ir(III)/Eu(III) dyads

When complexes **5a–5e** were used to study the ET process, the strong phosphorescence from the Ir complexes generated from the dissociation of the Ir–Eu complexes made it difficult to see obvious emissions from  $\text{Eu}^{3+}$  ions in the solutions (Fig. S1†), which is consistent with the previous studies.<sup>42,63</sup> Therefore, in order to decrease the emission from free Ir complex and get the obvious influence tendency of bridging ligands, we added  $\text{EuCl}_3$  into the solution of the complexes **4a–4e** (Ir/Eu = 1 : 1 molar ratio,  $10^{-5} \text{ M}$  in EtOH). Though at room temperature, no obvious emission was observed from  $\text{Eu}^{3+}$  and only weak emission from the iridium moieties (for **4a–4d**) was detected, intense emissions from both the iridium and europium moieties were observed for the **4a–4d**/Eu(III) dyads (Fig. 7 and Table 3) when the temperature was lowered to 77 K. As the triplet energy level of the bridging ligand decreases, the emission from the iridium moiety gradually weakens and that from the europium moiety becomes stronger. It

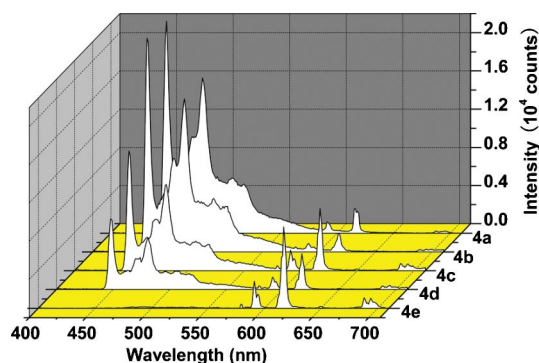


Fig. 7 Emission spectra of **4a–4e** with  $\text{EuCl}_3 \cdot 6\text{H}_2\text{O}$  (1 : 1,  $1 \times 10^{-5} \text{ M}$ ) at 77 K in EtOH glass.

is worth noting that, at 77 K, the **4e**/Eu(III) dyad exhibited pure red emission from the europium ions and emission from the iridium moiety was completely quenched. The reason for this is that the triplet energy level of ligand **2e** is lower than the  $^3\text{MLCT}$  level of  $\text{Ir}(\text{dfppy})_2^+$  but higher than the  $^5\text{D}_0$  energy levels of the  $\text{Eu}^{3+}$  ion with an energy gap of  $2.8 \times 10^3 \text{ cm}^{-1}$ , which is suitable for complete ET from  $\text{Ir}(\text{dfppy})_2^+$  of **4e** to the  $\text{Eu}^{3+}$  ion. Besides, the excitation spectra of the Ir(III)/Eu(III) dyads tracking the 613 nm emission of  $\text{Eu}^{3+}$  (Fig. S2†) show an obvious broad excitation character of corresponding iridium complex instead of the narrow excitation of  $\text{Eu}^{3+}$ , and the excitation intensity for **4e**/Eu(III) was much stronger than the other systems.

The excited-state lifetimes of the complexes **4a–4d** with and without  $\text{Eu}^{3+}$  ions were measured at 77 K. All of the decay curves were fitted with monoexponential functions, giving reliable  $\chi^2$  (see Table 3), meaning that there is only one kind of emissive species corresponding to each emission band. The lifetimes of complexes **4a–4d** range between 4.5 and 5.0  $\mu\text{s}$ , which are typical for phosphorescence. However, after  $\text{Eu}^{3+}$  was added, the lifetimes of the iridium moieties decreased obviously for the systems containing complexes **4a–4d**, which further confirms that ET from the Ir moieties to the  $\text{Eu}^{3+}$  ions took place.<sup>41</sup>

The ET process from complexes **4a–4e** to the europium ions is summarized schematically in Fig. 8. Firstly, the iridium complex was excited to the  $^1\text{MLCT}$  state, which quickly transformed to the  $^3\text{MLCT}$  state through intersystem crossing because of strong spin-orbit coupling. Energy from both the excited  $^3\text{MLCT}_1$  and  $^3\text{MLCT}_2$  levels can transfer to the triplet energy levels of the linking ligand. For complex **4e**, the transfer process is complete due to the match of the energy levels, and then energy transferred from **2e** to

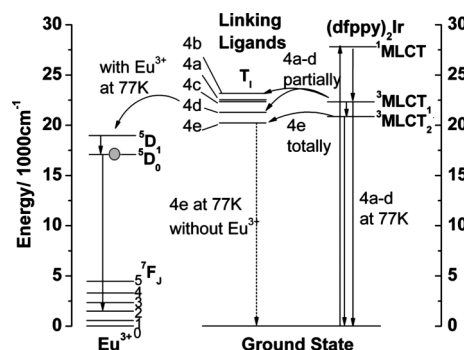


Fig. 8 Schematic representation of the ET processes in the Ir–Eu systems.

the  $^5D_J$  level of the  $\text{Eu}^{3+}$  ion generates pure red emission. However, in the other four systems, mixed emission was observed because of the incomplete energy transfer from the excited  $^3\text{MLCT}$  state to the triplet energy levels of **2a–2d**, as well as possible reverse transfer. Therefore, the triplet energy level of the linking ligand is important, because it behaves as a channel for ET in the above Ir–Eu dyads. Complete ET will occur only when the triplet energy level of the linking ligand is suitably lower than the  $^3\text{MLCT}$  level of the Ir moiety and higher than the  $^5D_J$  levels of the  $\text{Eu}^{3+}$  ion, resulting in efficient sensitization.

## Conclusions

The synthesis and characterization of Ir(III) complexes of a series of  $\text{N}^{\wedge}\text{N},\text{O}^{\wedge}\text{O}$ -chelating linking ligands based on substituted 1-(pyridin-2-yl)-3-methyl-5-pyrazolone was reported. The ET process between these iridium complexes and europium ions in solution was investigated. The triplet energy level of the linking ligand is a key factor in terms of the ET process between the two emission centers. Only when the triplet energy level of the linking ligand is sufficiently lower than the  $^3\text{MLCT}$  energy levels of the Ir moiety and higher than the  $^5D_J$  energy levels of the  $\text{Eu}(\text{III})$  ion will complete ET occur and pure emission from the  $\text{Eu}(\text{III})$  ion be observed (for example, **4e**). If the triplet energy level of the linking ligand is higher or close to the  $^3\text{MLCT}$  energy levels of the Ir moiety, mixed emission from both the Ir moiety and the  $\text{Eu}(\text{III})$  moiety (**4a–4d**) is obtained. These findings could be helpful in the design of linking ligands for sensitizing europium ions.

## Acknowledgements

The authors thank the National Basic Research Program (2006CB601103) and the NNSFC (90922004, 20971006, 20821091, and 50772003) for financial support as well as beamline BL14W (Shanghai Synchrotron Radiation Facility) for providing the beam time.

## References

- 1 D. Parker, *Coord. Chem. Rev.*, 2000, **205**, 109–130.
- 2 L. J. Charbonniere, R. Ziessel, M. Montalti, L. Prodi, N. Zaccheroni, C. Boehme and G. Wipff, *J. Am. Chem. Soc.*, 2002, **124**, 7779–7788.
- 3 R. K. Mahajan, I. Kaur, R. Kaur, S. Uchida, A. Onimaru, S. Shinoda and H. Tsukube, *Chem. Commun.*, 2003, 2238–2239.
- 4 T. Gunnlaugsson, J. P. Leonard, K. Senechal and A. J. Harte, *J. Am. Chem. Soc.*, 2003, **125**, 12062–12063.
- 5 T. Gunnlaugsson, J. P. Leonard, K. Senechal and A. J. Harte, *Chem. Commun.*, 2004, 782–783.
- 6 T. Terai, K. Kikuchi, S. Y. Iwasawa, T. Kawabe, Y. Hirata, Y. Urano and T. Nagano, *J. Am. Chem. Soc.*, 2006, **128**, 6938–6946.
- 7 N. Shao, J. Y. Jin, G. L. Wang, Y. Zhang, R. H. Yang and J. L. Yuan, *Chem. Commun.*, 2008, 1127–1129.
- 8 Q. P. Qin, T. Lovgren and K. Pettersson, *Anal. Chem.*, 2001, **73**, 1521–1529.
- 9 F. B. Wu, S. Q. Han, C. Zhang and Y. F. He, *Anal. Chem.*, 2002, **74**, 5882–5889.
- 10 P. von Lode, J. Rosenberg, K. Pettersson and H. Takalo, *Anal. Chem.*, 2003, **75**, 3193–3201.
- 11 T. Kokko, L. Kokko, T. Lovgren and T. Soukka, *Anal. Chem.*, 2007, **79**, 5935–5940.
- 12 S. V. Eliseeva and J. C. G. Bunzli, *Chem. Soc. Rev.*, 2010, **39**, 189–227.
- 13 J. Kido, H. Hayase, K. Hongawa, K. Nagai and K. Okuyama, *Appl. Phys. Lett.*, 1994, **65**, 2124–2126.

- 14 C. Adachi, M. A. Baldo and S. R. Forrest, *J. Appl. Phys.*, 2000, **87**, 8049–8055.
- 15 Z. R. Hong, C. J. Liang, R. G. Li, W. L. Li, D. Zhao, D. Fan, D. Y. Wang, B. Chu, F. X. Zang, L. S. Hong and S. T. Lee, *Adv. Mater.*, 2001, **13**, 1241–1245.
- 16 F. S. Liang, Q. G. Zhou, Y. X. Cheng, L. X. Wang, D. G. Ma, X. B. Jing and F. S. Wang, *Chem. Mater.*, 2003, **15**, 1935–1937.
- 17 T. Oyamada, Y. Kawamura, T. Koyama, H. Sasabe and C. Adachi, *Adv. Mater.*, 2004, **16**, 1082–1086.
- 18 P. P. Sun, J. P. Duan, J. J. Lih and C. H. Cheng, *Adv. Funct. Mater.*, 2003, **13**, 683–691.
- 19 H. You and D. G. Ma, *J. Phys. D. Appl. Phys.*, 2008, **41**.
- 20 F. S. Richardson, *Chem. Rev.*, 1982, **82**, 541–552.
- 21 J. C. G. Bunzli and C. Piguet, *Chem. Soc. Rev.*, 2005, **34**, 1048–1077.
- 22 S. I. Weissman, *J. Chem. Phys.*, 1942, **10**, 214–217.
- 23 H. Xin, F. Y. Li, M. Shi, Z. Q. Bian and C. H. Huang, *J. Am. Chem. Soc.*, 2003, **125**, 7166–7168.
- 24 M. Shi, F. Y. Li, T. Yi, D. Q. Zhang, H. M. Hu and C. H. Huang, *Inorg. Chem.*, 2005, **44**, 8929–8936.
- 25 S. Biju, D. B. A. Raj, M. L. P. Reddy, C. K. Jayasankar, A. H. Cowley and M. Findlater, *J. Mater. Chem.*, 2009, **19**, 1425–1432.
- 26 S. Biju, M. L. P. Reddy, A. H. Cowley and K. V. Vasudevan, *Cryst. Growth Des.*, 2009, **9**, 3562–3569.
- 27 S. Biju, M. L. P. Reddy, A. H. Cowley and K. V. Vasudevan, *J. Mater. Chem.*, 2009, **19**, 5179–5187.
- 28 W. F. Sager, Filipesc. N and F. A. Serafin, *J. Phys. Chem.*, 1965, **69**, 1092–1100.
- 29 F. J. Steemers, W. Verboom, D. N. Reinhoudt, E. B. Vandertol and J. W. Verhoeven, *J. Am. Chem. Soc.*, 1995, **117**, 9408–9414.
- 30 M. Latva, H. Takalo, V. M. Mikkala, C. Matachescu, J. C. Rodriguez-Ubis and J. Kankare, *J. Lumin.*, 1997, **75**, 149–169.
- 31 L. M. Fu, X. C. Ai, M. Y. Li, X. F. Wen, R. Hao, Y. S. Wu, Y. Wang and J. P. Zhang, *J. Phys. Chem. A*, 2010, **114**, 4494–4500.
- 32 S. Comby and J. C. G. Bunzli, ed., *Handbook on the Physics and Chemistry of Rare Earths*, North-Holland Publishing Co., Amsterdam, 2007.
- 33 T. A. Miller, J. C. Jeffery, M. D. Ward, H. Adams, S. J. A. Pope and S. Faulkner, *Dalton Trans.*, 2004, 1524–1526.
- 34 D. Imbert, M. Cantuel, J. C. G. Bunzli, G. Bernardinelli and C. Piguet, *J. Am. Chem. Soc.*, 2003, **125**, 15698–15699.
- 35 S. J. A. Pope, B. J. Coe and S. Faulkner, *Chem. Commun.*, 2004, 1550–1551.
- 36 S. J. A. Pope, B. J. Coe, S. Faulkner, E. V. Bichenkova, X. Yu and K. T. Douglas, *J. Am. Chem. Soc.*, 2004, **126**, 9490–9491.
- 37 N. M. Shavaleev, L. P. Moorcraft, S. J. A. Pope, Z. R. Bell, S. Faulkner and M. D. Ward, *Chem.–Eur. J.*, 2003, **9**, 5283–5291.
- 38 S. I. Klink, H. Keizer, H. W. Hofstraat and F. van Veggel, *Synth. Met.*, 2002, **127**, 213–216.
- 39 S. I. Klink, H. Keizer and F. van Veggel, *Angew. Chem., Int. Ed.*, 2000, **39**, 4319–4321.
- 40 D. Guo, C. Y. Duan, F. Lu, Y. Hasegawa, Q. J. Meng and S. Yanagida, *Chem. Commun.*, 2004, 1486–1487.
- 41 P. Coppo, M. Duati, V. N. Kozhevnikov, J. W. Hofstraat and L. De Cola, *Angew. Chem., Int. Ed.*, 2005, **44**, 1806–1810.
- 42 F. F. Chen, Z. Q. Bian, Z. W. Liu, D. B. Nie, Z. Q. Chen and C. H. Huang, *Inorg. Chem.*, 2008, **47**, 2507–2513.
- 43 T. D. Pasatou, A. M. Madalan, M. U. Kumke, C. Tiseanu and M. Andruh, *Inorg. Chem.*, 2010, **49**, 2310–2315.
- 44 F. F. Chen, Z. Q. Chen, Z. Q. Bian and C. H. Huang, *Coord. Chem. Rev.*, 2010, **254**, 991–1010.
- 45 M. Cantuel, F. Gummy, J. C. G. Bunzli and C. Piguet, *Dalton Trans.*, 2006, 2647–2660.
- 46 P. B. Glover, P. R. Ashton, L. J. Childs, A. Rodger, M. Kercher, R. M. Williams, L. De Cola and Z. Pikramenou, *J. Am. Chem. Soc.*, 2003, **125**, 9918–9919.
- 47 M. S. Lowry and S. Bernhard, *Chem.–Eur. J.*, 2006, **12**, 7970–7977.
- 48 P. Lian, H. B. Wei, C. Zheng, Y. F. Nie, J. Bian, Z. Q. Bian and C. H. Huang, *Dalton Trans.*, 2011, **40**, 5476–5482.
- 49 S. Sprouse, K. A. King, P. J. Spellane and R. J. Watts, *J. Am. Chem. Soc.*, 1984, **106**, 6647–6653.
- 50 W. Y. Wong, G. J. Zhou, X. M. Yu, H. S. Kwok and Z. Y. Lin, *Adv. Funct. Mater.*, 2007, **17**, 315–323.
- 51 A. Cingolani, Effendy, F. Marchetti, C. Pettinari, R. Pettinari, B. W. Skelton and A. H. White, *Inorg. Chem.*, 2004, **43**, 4387–4399.
- 52 Y. M. You and S. Y. Park, *J. Am. Chem. Soc.*, 2005, **127**, 12438–12439.

- 53 P. Coppo, E. A. Plummer and L. De Cola, *Chem. Commun.*, 2004, 1774–1775.
- 54 F. O. Garces, K. A. King and R. J. Watts, *Inorg. Chem.*, 1988, **27**, 3464–3471.
- 55 F. F. Chen, Z. Q. Bian, B. Lou, E. Ma, Z. W. Liu, D. B. Nie, Z. Q. Chen, J. Bian, Z. N. Chen and C. H. Huang, *Dalton Trans.*, 2008, 5577–5583.
- 56 B. Ravel and M. Newville, *J. Synchrotron Radiat.*, 2005, **12**, 537–541.
- 57 E. Orselli, G. S. Kottas, A. E. Konradsson, P. Coppo, R. Frohlich, R. Frtshlich, L. De Cola, A. van Dijken, M. Buchel and H. Borner, *Inorg. Chem.*, 2007, **46**, 11082–11093.
- 58 S. Lamansky, P. Djurovich, D. Murphy, F. Abdel-Razzaq, H. E. Lee, C. Adachi, P. E. Burrows, S. R. Forrest and M. E. Thompson, *J. Am. Chem. Soc.*, 2001, **123**, 4304–4312.
- 59 Z. W. Liu, D. B. Nie, Z. Q. Bian, F. F. Chen, B. Lou, J. Bian and C. H. Huang, *ChemPhysChem*, 2008, **9**, 634–640.
- 60 C. Reinhard and H. U. Gudel, *Inorg. Chem.*, 2002, **41**, 1048–1055.
- 61 Z. F. Li, J. B. Yu, L. Zhou, H. J. Zhang, R. P. Deng and Z. Y. Guo, *Org. Electron.*, 2008, **9**, 487–494.
- 62 T. Holstein, S. K. Lyo and R. Orbach, *Phys. Rev. B: Solid State*, 1977, **16**, 934–942.
- 63 D. Sykes and M. D. Ward, *Chem. Commun.*, 2011, **47**, 2279–2281.